On physical mechanisms in chemical reaction-driven tip-streaming

R. Krechetnikov and G. M. Homsy
University of California, Santa Barbara, California 93106

In this work we provide a basic physical modeling of the spatiotemporal pattern of emulsification produced by chemical reaction-driven tip-streaming and observed by Fernandez and Homsy [Phys. Fluids **16**, 2548 (2004)]. Features of this phenomenon—nonlinear autooscillations, a conical drop shape, tip-streaming, and droplet trajectory splitting—are addressed in this paper. In particular, the experimentally found regimes of self-sustained periodic motion and the transitions between them are explained with the help of a nonlinear relaxation oscillator model. An exact self-similar solution for the steady tip-streaming mode supports the suggested mechanism of a Marangoni-driven phenomenon. Finally, the ionic nature of the surfactant produced at the interface offers a reasonable explanation for the formation of a spray cone, which is due to repulsive electrostatic interactions between droplets. These features distinguish this phenomenon from standard tip-streaming. © *2004 American Institute of Physics.* [DOI: 10.1063/1.1739232]

I. INTRODUCTION AND BASIC PHENOMENA DESCRIPTION

The phenomenon to be discussed here was discovered by Fernandez and Homsy[1] in the course of pendant drop measurements conducted to determine the interfacial tension (IFT). Experimental observations were done under conditions of an acid/alkaline reaction taking place at the oil/water interface. This particular reaction is well studied in view of its importance in oil recovery,[2] since a low IFT resulting from the production of the surface active substance enhances this processes (cf. Donnan).[3] Thus, even though the pendant drop method[4] has been extended to transient and dynamic IFT measurements,[5] the discovered phenomena reveals its limitations, since the usual method assumes a uniform distribution of the surfactant along the interface.[6] As we will see, the phenomena imply the existence of significant concentration gradients.

The observed phenomenon involves three main features: (1) tip-streaming—the formation of a conical drop shape with pointed ends [cf. Fig. 1(c)] and ejection of very small, 4 μm, droplets [cf. Fig. 2(a)] from the pointed ends; (2) nonlinear self-sustained oscillations—a periodic change of the drop shape from nearly hemispherical [Fig. 1(a)] to conical [Fig. 1(c)]; (3) droplet separation—an organized motion, in which one ejected droplet moves to the right, while the subsequent one moves to the left [cf. Figs. 2(a)–2(b)].

The first effect (tip-streaming), to the authors' knowledge, has never been observed in systems with internal chemically driven flows, but readily occurs in externally imposed shear or extensional flows, like the four-roll mill device.[7] While a complete theoretical understanding of the tip-steaming phenomena is still lacking, its basic features are quite extensively studied experimentally (cf. the recent review by Stone).[8] Starting with experiments by Taylor,[7] it is known that drops with low viscosity relative to the ambient fluid, i.e., with viscosity ratio $\lambda < O(0.1)$, can lead to the tip-streaming. Later experimental studies by de Bruijn[9] in simple shear flows distinguished two primary modes of drop breakup: a *fracture* mode occurring for pure fluids at a certain shear rate (equivalently, at a critical capillary number Ca_c), accompanied by the formation of satellite droplets; and *tip-streaming*, which takes place in the presence of surfactants and produces much smaller drops without satellites. The shear rates required for the last type of breakup in simple shear flows can be 2 orders of magnitude lower than for the fracture mode. In the case of extensional (straining) flows, the presence of surfactant may also significantly lower the critical capillary number (cf. Siegel[10] and Hu *et al.*[11]) from that for pure fluids studied by Acrivos and Lo.[12] While the effect of surfactants appears to lower Ca_c, the limits of low (dilute) and high (saturated) concentrations of surfactant leads to Ca_c corresponding to the pure liquid case as long as the relevant value of IFT is used. The last fact indicates the importance of surfactant gradients in the tip-steaming phenomena as elucidated by de Bruijn[9] for simple shear flows and by Eggleton *et al.*[13,14] for extensional flows. However, the role of surfactant concentration gradients is yet not fully understood and thus admits alternative hypotheses. In particular, a qualitative explanation of the effect of surfactants in lowering critical capillary number given by de Bruijn[9] and Stone[8] is based on assumption of rigid ends of the drop due to swept surfactant, so that viscous stresses required for tearing the narrow regions away are lower. However, this explanation should remain valid at saturation concentrations as
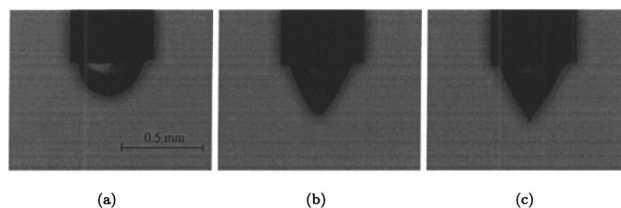

FIG. 1. Nonlinear oscillations of a pendant drop shape: from hemispherical (a) to conical (c) (courtesy of J. Fernandez).
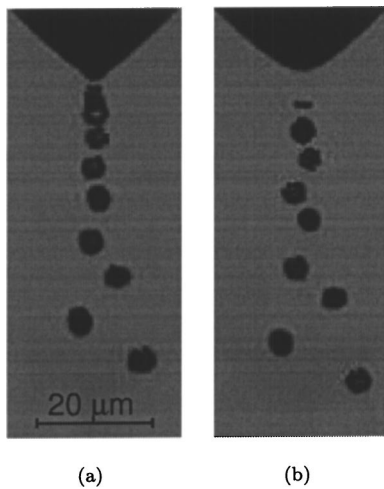
FIG. 2. Tip-streaming and droplet separation (courtesy of J. Fernandez).

well, thus contradicting experimental observations and emphasizing the importance of surfactant gradients.

Our hypothesis, shown in Fig. 3, refers to capillary breakup of a cylindrical jet. First, consider a clean interface case depicted in Fig. 3(a). Axisymmetric longitudinal disturbances inevitably yield "trough" and "crest" regions. The capillary forces in the trough regions tend to collapse the interface with a force F_c, while the forces F_r which tend to restore the cylindrical shape, have a radial component F_r' that competes with F_c. If the wavelength of instability is large enough, $\lambda > 2\pi a$, with a being a radius of the undisturbed cylinder, F_r' cannot balance F_c and collapse takes place.

This standard understanding of Rayleigh jet breakup indicates that when: (i) the tip of a thread is saturated with surfactant as shown in Fig. 3(b) and (ii) there are gradients in surfactant concentration (surface tension to the left of the tip is higher), the restoring force F_r and its radial component F_r' are much weaker in view of the lower surface tension. This fact allows for much shorter unstable wavelengths, as found experimentally in Ref. 1, and for the smaller size of the droplets, which becomes close to the diameter of the thread. While this picture is based on static reasoning, dynamics comes into the mechanism of accumulation of surfactant in the tip region.

In systems which contain only a small amount of contaminant, tip-streaming stops when most of the surfactant is swept away, while systems with surfactant solutions can exhibit ever-continuing tip-streaming. Our system belongs to the latter class, because the chemical reaction provides a constant supply of surfactant, at least until the reactants are depleted.

It is worthwhile mentioning the apparent similarity of the observed cone shape of the drop in the bursting regime to Taylor cones.[15,16] While the shape and bursting effects suggest an analogy to the phenomena of formation of stable cones in electrified liquid interfaces, the underlying physical mechanisms are different. As explained by Taylor (who assumed equipotentiality of the interface), the conical shape arises as a balance of normal stresses: the electrostatic pressure $p_E = \frac{1}{2}\epsilon_0 E_n^2$ induced by the normal component of electrical field E_n (the tangential component being zero in view of equipotentiality) equilibrates with the capillary pressure $p_\sigma = \sigma \cot \alpha / r$ which varies inversely with the distance from cone tip, r, so that $E_n \sim (\sigma/\epsilon_0 r)^{1/2}$. In the case of gradients of the interfacial potential, the tangential component of electrical stresses $\sim \epsilon_0 E_n E_\tau$ can be either negligible or lead to swirling or nonswirling motion inside the Taylor cone (cf. Hayati et al.)[17] without influencing its self-similar conical shape. In our case, the conical shape is produced as a result of balancing both normal and tangent stresses, so that the predominant role is played by the gradient of surface tension. As a result, the cone shape results from nontrivial fluid motion both inside (which is analogous to that produced in Taylor cones by tangential stresses) and outside the cone.

The mechanism explaining the second effect (nonlinear self-sustained oscillations) consists of the basic sequence, triggered by (t) the *first drop effect*, named here in analogy with the first drop effect in the dripping faucet—detachment of a large drop under gravity leading to an extensional flow in the viscous oil. Under usual circumstances, this flow would attenuate due to viscous dissipation, but in this particular case it leads to: (i) sweeping surfactant towards the tip of a new pendant drop and, if the viscous extensional flow produced by the *first drop effect* is strong enough, deforming the interface up to formation of a pointed end, and (ii) bursting. The bursting (tip-streaming) in turn removes surfactant from the tip of the drop, and (iii) the surfactant concentration gradient between the top and the tip of the drop so created (sketched in Fig. 4) drives a Marangoni flow, which (iv) has the same effect as the *first drop*. Thus one has the following sequence: $(t) \rightarrow (i) \rightarrow (ii) \rightarrow (iii) \rightarrow (iv) \rightarrow (i) \rightarrow (ii) \rightarrow (iii) \rightarrow (iv) \rightarrow \dots$. The experiments revealed two particular modes of this process: nonlinear self-sustained oscillations of the drop and steady tip-streaming, when there is no apparent time dependence of the nearly conical shape of the remaining pendant drop. See Fernandez and Homsy[1] for a detailed description.

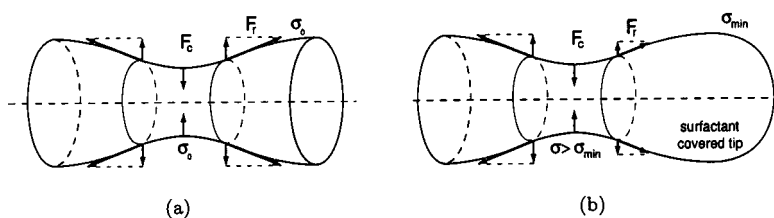Nonlinear self-sustained oscillations have been found

FIG. 3. The role of surfactant in the phenomena of tip-streaming. (a) Breakup of a clean interface Rayleigh jet. (b) Breakup of a surfactant covered thread.
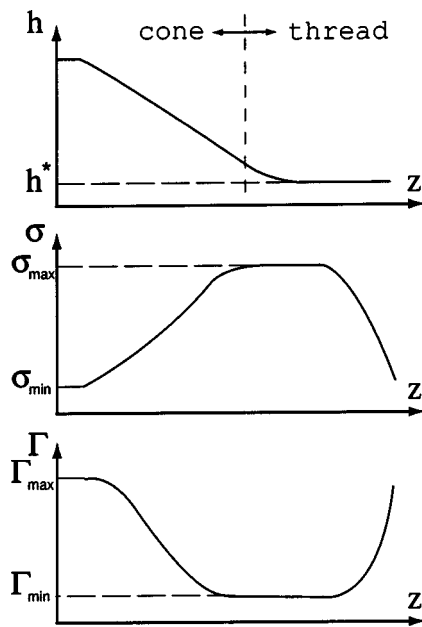
FIG. 4. Sketch of the driving mechanism.

previously in different circumstances involving chemical reactions that produce surfactants. In particular, Dupeyrat and Nakashe[18] observed a macroscopic self-agitation in a quasi-periodic variation of interfacial tension in an oil/water system, in which a cationic surfactant is dissolved in the aqueous phase. Magone and Yoshikawa[19] studied the analogous system of an oil droplet situated in an aqueous layer of surfactant solution. The proposed mechanism for these self-sustained oscillations consists of a gradual formation of an interfacial monolayer of surfactant until a critical value of surface pressure is reached, followed by monolayer collapse and cationic surfactant migration into the bulk. This leads to an abrupt decrease of IFT and, therefore to the macroscopic motion of the drop accompanied by the change of the curvature of a certain part of the interface. As the monolayer forms again, the phenomenon repeats itself for 30–60 min. Another example of autooscillations was observed by Kovalchuk et al.[20] in a system where a droplet of a surfactant solution with limited solubility on a tip of a capillary under a free liquid surface dissolves in a container. The autooscillations in this case are attributed to a competition between diffusion and convection transport of the surfactant.

In general, nonlinear Marangoni-driven oscillations can be due to either concentration[20] or temperature gradients.[21] Our phenomenon belongs to the last subclass, when the surfactant is produced by chemical reaction.[18,19] The only difference from previous works[18,19] consists of developing a singularity at the interface which leads to surfactant transfer by tip-streaming. We develop a simple mass-spring mechanical model which predicts both modes of tip-streaming described above. In the model formulation we followed the same lines as in the analysis of a dripping faucet.[22,23] The similarity of these two phenomena consists of nonlinear oscillations and singularity formation. However, the objectives in the analysis of the mechanical model of the dripping faucet are centered around its chaotic behavior, since after the

original conjecture by Rössler,[24] it was found that its time delay diagrams exhibit period doubling and chaos as the flow rate changes. With a few recent exceptions, numerous works (cf. de Innocento and Renna[25] and references therein) on this relatively simple system[26] are restricted to a relaxation oscillator (cf. original works by Shaw and Martien et al.)[23]—a phenomenologically motivated equation—instead of treating the hydrodynamics in a rational way. Rational models became possible due to the one dimensional slender-jet approximation of the axisymmetric Navier–Stokes equations,[27] and an approximate overall energy description in Lagrangian variables.[28,29] Neither of these approaches is applicable in our case for obvious reasons. As a result, we follow the historical way of model development starting with the simplest mechanical model. Of course, this approach does not provide any details on the shape and pinch-off, but nevertheless gives important insight into the basic physical processes.

The third effect (droplet trajectory splitting) is the most subtle one, which makes this particular tip-streaming different from the classical one (in which the jet is ejected along the extensional axis and droplets do not experience any kind of trajectory splitting). Our hypothesis in explaining this phenomenon is based on the ionic nature of the surfactant, which, in view of particular size of the pendant drop and droplets, provides a repulsive electrostatic interaction sufficient to explain the experimentally observed speeds of the sideways motion of droplets.

The paper is organized as follows. In Sec. II we provide the general set of governing parameters, their magnitude, and their role in the phenomena. Then we perform a basic overall energy analysis and formulate and analyze a mechanical model of nonlinear oscillations. In the second part of this section we deduce a self-similar solution which helps to understand the flow pattern when tip-streaming takes place. It also happens to be important in the discussion of the electrokinetic mechanism of droplet trajectory splitting, to which Sec. III is devoted.

II. PENDANT DROP DYNAMICS

We first identify the characteristic nondimensional parameters which govern the behavior of the system. Since the system does not involve any external mechanical motion, but nevertheless exhibits observable macroscopic motion, one needs to define the characteristic speed, U_0, and Weber (or effective Reynolds) number

$$\text{We} = \frac{\rho U_0^2 D}{\sigma_0} \Leftrightarrow \text{Re} = \frac{\rho U_0 D}{\mu}. \tag{1}$$

As it is easy to deduce from the analysis of Marangoni-driven flow due to a surface tension gradient, the boundary layer near the interface of some characteristic length D, which is here understood as the pendant drop diameter 0.4 mm, has the following scales for the thickness and speed:

$$\delta \sim D \left(\frac{\mu^2}{D\sigma_0} \right)^{1/3}, \quad U_0 \sim \frac{\delta}{D} \frac{\sigma_0}{\mu}, \tag{2}$$

Phys. Fluids, Vol. 16, No. 7, July 2004

On physical mechanisms   2559

TABLE I. Basic physical constants (at $T = 20\,°C$).

Interfacial tension σ_0	35 mN/m
Dynamic viscosity of water μ_w	1.002 mPa s
Dynamic viscosity of oil μ_o	0.22 Pa s
Density of water ρ_w	998 kg/m^3
Density of oil μ_o	764 kg/m^3
Kinetic rate constant k^{a}	0.29 m^3 mol^{-1} s^{-1}
Bulk concentration $C_{\mathrm{RO^-H^+}}$	1.0 mol/m^3
Bulk concentration C_{NaOH}	12.5 mol/m^3
Surface-excess concentration $\Gamma_{\max}$	10^{-5} mol/m^2

[a]Reference 5.

where σ_0 is a reference interfacial tension, and μ the dynamic viscosity. With such a scaling for U_0 one can estimate the effective Reynolds number. In Table I we provide a list of relevant physical constants and their magnitudes (for details refer to Ref. 1).

Using these numbers, one finds that the flow in the water phase is of a boundary layer type with $U_w \sim 35$ m/s and $We_w \sim 10^4$, while the flow in the oil phase is of moderate Reynolds number, so that $U_o \sim 0.15$ m/s and $We_o \sim 0.2$. It should be noted that U_o is of the order of the speed of the droplets ejected due to tip-streaming. Subsequently, the shear rate in the oil phase is estimated as

$$G \sim \frac{U_o}{D} \sim 10^2 \text{ s}^{-1}, \tag{3}$$

which is of the order of that observed experimentally.[1] The above parameters characterize the hydrodynamic properties of the system. Its chemical properties, important for our purposes, are best described by the production rate constant R_0 which follows from nonequilibrium Langmuir-type sorption kinetics[30]

$$\frac{d\Gamma_{\mathrm{RO^-}}}{dt} = k\Gamma_{\max}\left[C_{\mathrm{RO^-}}\left(1 - \frac{\Gamma_{\mathrm{RO^-}}}{\Gamma_{\max}}\right) - \frac{1}{K_{\mathrm{eq}}}\frac{\Gamma_{\mathrm{RO^-}}}{\Gamma_{\max}}\right], \tag{4}$$

where k is a kinetic rate constant, K_{eq} an equilibrium constant, $C_{\mathrm{RO^-}}$ the bulk-phase concentration at the interface, $\Gamma_{\mathrm{RO^-}}$ the surface-excess concentration, and $\Gamma_{\max}$ the surface-excess saturation concentration. Therefore, the production rate is estimated as $R_0 \simeq k\Gamma_{\max}C_{\mathrm{RO^-}} = 0.29 \times 10^{-5}$ mol m^{-2} s^{-1} and $\Gamma_{\max}/R_0$ essentially represents a characteristic time scale.

In order to understand the complexity of the phenomenon it is sufficient to look at the energy balance for the whole system. Neglecting the effect of a free (gas–liquid) surface and assuming $|\rho^{(2)} - \rho^{(1)}| \ll \rho^{(1,2)}$, the energy balance reads (with the standard notation)

$$\frac{d}{dt}\left[\int_V \frac{\rho|\mathbf{v}|^2}{2}dV + \int_A \sigma\, dA - \int_V \varphi\, dV\right]$$

$$= -\int_V \tau \cdot (\nabla\mathbf{v})dV \tag{5}$$

$$+ \int_A \left\{\frac{d\sigma}{d\Gamma}(f + \mathbf{v}\cdot\nabla_s\Gamma - \Gamma\nabla_s\cdot\mathbf{v}) + \sigma\nabla_s\cdot\mathbf{v}_s\right\}dA, \tag{6}$$

where the left-hand side represents a sum of kinetic and potential energy (surface tension and gravitation with $\varphi = \rho g e_k x_k$ being a potential), the first term on the right-hand side is a viscous dissipation term (τ is the viscous stress tensor), while the remaining terms provide an energy supply due to production f of surfactant of concentration Γ as well as energy storage and dissipation due to surface stretching $\nabla_s \cdot \mathbf{v}_s$, inflation $\nabla_s \cdot \mathbf{v}_n$, and surfactant transport. Given the complexity, it is not feasible to perform reliable phenomenological modeling of these terms as done, for example, in the problems of a liquid drop spreading on a solid surface[31] and of the damping of shape oscillations of liquid drops.[32] Therefore we pursue a classical mechanical approach in order to predict the basic properties of the phenomena.

A. Relaxation oscillator model

In analogy with the simple mechanical model for the dripping faucet proposed by Martien et al.[23] we formulate the dynamics of the pendant drop in terms of the evolution of a geometric point x at the axis of symmetry, at which one can apply Newton's second law. This model consists of a mass of the pendant drop M, pulling on a spring with a spring constant k. We take $M \sim \pi D^3 \rho/12$ in view of the added mass effect, and for simplicity we neglect the change of pendant drop mass due to droplet ejection, which corresponds to a quasisteady approximation. This is justified by the 2 orders of magnitude difference between sizes of the droplets; $d = 6\,\mu$m, and the pendant drop $D = 0.4$ mm. Since the pressure difference between the inside and outside of the drop $\sim \sigma D$ and $\delta x \sim D$, we conclude that $k(\Gamma)$ has the meaning of a surface tension and is approximated here by a simple state equation $k(\Gamma) = \sigma_0 \cdot (1 - \Gamma/\Gamma_{\max})$.[33] For the forcing we assume the surfactant concentration to grow linearly with time with chemical reaction rate R, which is a control parameter in our case. The forces involved include: gravity, Mg with $g \simeq 9.8$ m s^{-2} being the gravitational acceleration, friction due to the fact that the fluid is viscous, $-b(dx/dt)$, with b as a friction coefficient, and a linear restoring force $-kx$ produced by the spring. When the surfactant concentration Γ reaches a critical value Γ_c, its magnitude is suddenly reduced by $\Delta\Gamma$, which in reality is a function of Γ_c, x_c, but for simplicity we use $\Delta\Gamma = \Gamma_c$, which implies that all surfactant is removed in the process of tip-streaming. The resulting mathematical model reads

$$M\frac{d^2x}{dt^2} = \underbrace{Mg}_{\text{gravity}} - \underbrace{b\frac{dx}{dt}}_{\text{friction}} - \underbrace{k(\Gamma)x}_{\text{surface tension}}, \tag{7}$$

$$\frac{d\Gamma}{dt} = R, \quad \text{when } \Gamma < \Gamma_c, \tag{8}$$

$$\Gamma = \Gamma_c - \Delta\Gamma, \quad \text{when } \Gamma = \Gamma_c. \tag{9}$$

The difference between our model and the ''dripping faucet'' problem is a discontinuity of a spring constant as opposed to mass; hence, the reaction rate is a control parameter instead of flow rate. Using the following scalings:

$$\Gamma \rightarrow \Gamma_{max}\Gamma, \quad t \rightarrow \frac{\Gamma_{max}}{R}t, \quad x \rightarrow Dx, \tag{10}$$

we arrive at the nondimensional version of the oscillator model

$$\left(\frac{R}{R_0}\right)^2 \frac{d^2x}{dt^2} + c_1\left(\frac{R}{R_0}\right)\frac{dx}{dt} + c_2 k(\Gamma)x = c_3, \tag{11}$$

$$\frac{d\Gamma}{dt} = R, \quad \text{when} \quad \Gamma < \Gamma_c, \tag{12}$$

$$\Gamma = \Gamma_c - \Delta\Gamma, \quad \text{when} \quad \Gamma = \Gamma_c, \tag{13}$$

where the reference reaction rate R_0 is defined above and the constants

$$c_1 = \frac{\Gamma_{max}b}{R_0 M}, \quad c_2 = \frac{\Gamma_{max}^2 \sigma_0}{R_0^2 M}, \quad c_3 = \frac{\Gamma_{max}^2 g}{R_0^2 D} \tag{14}$$

are estimated as $c_1 = 10^4$, $c_2 = 10^7$, and $c_3 = 2 \times 10^5$. The ratio R/R_0 is taken as the physical control parameter, which can be changed by different means, e.g., by varying the concentrations or reactants.

System (11) has been integrated numerically for a wide range of the parameter $R/R_0 \in [1, 2000]$ with the discontinuous surface excess behavior shown in Fig. 5(a) producing four general types of dynamics of the pendant drop:

(1) *Slow reaction*, $R/R_0 = 1$. Gradual stretching of the drop occurs until Γ reaches saturation, followed by a (quite stiff) relaxation to the original equilibrium shape, as shown in Fig. 5(b). The time scale of the nonlinear oscillations is identical to the period of discontinuous oscillations of Γ and, for the conditions of Table I, has an estimate

$$T = \Gamma_{max}/R \sim 3 \text{ s}. \tag{15}$$

(2) *Moderately fast reaction*, $R/R_0 = 100$. This regime still exhibits oscillations, but an increase of reaction rate leads to smoothing of the relaxation part of the oscillations, as shown in Fig. 5(c).

(3) *Very fast reaction*, $R/R_0 = 2000$. A further increase of R leads to a *quasisteady tip-streaming* state, so that the shape is distorted just slightly, as shown in Fig. 5(d), with the amount of the removed surfactant being fixed. The observed size and quantity of droplets is the same as in the nonlinear oscillation regime. Physically, this situation corresponds either to $\sigma \approx 0$ over the major part of the cone and a Marangoni flow localized around thread region, or to the macroscopic Marangoni flow under conditions that the adsorption flux to the interface and the flux due to tip-streaming are of the same order.

(4) *Very fast reaction*, $R/R_0 = 2000$, no dissipation, $c_1 \ll 1$. In the situation analogous to (3), but with negligible dissipation, one can observe pendant drop oscillations with a period which is much larger than that of Γ, as one can observe in Fig. 5(e). Physically, the reduced dissipation can be reached either by the lowering of the ambient liquid viscosity, or by switching to mode (3), since the absence of the macroscopic oscillations also leads to friction reduction.

For comparison we provide the experimental data on the evolution of the tip position with time in Fig. 6. The oscilla-
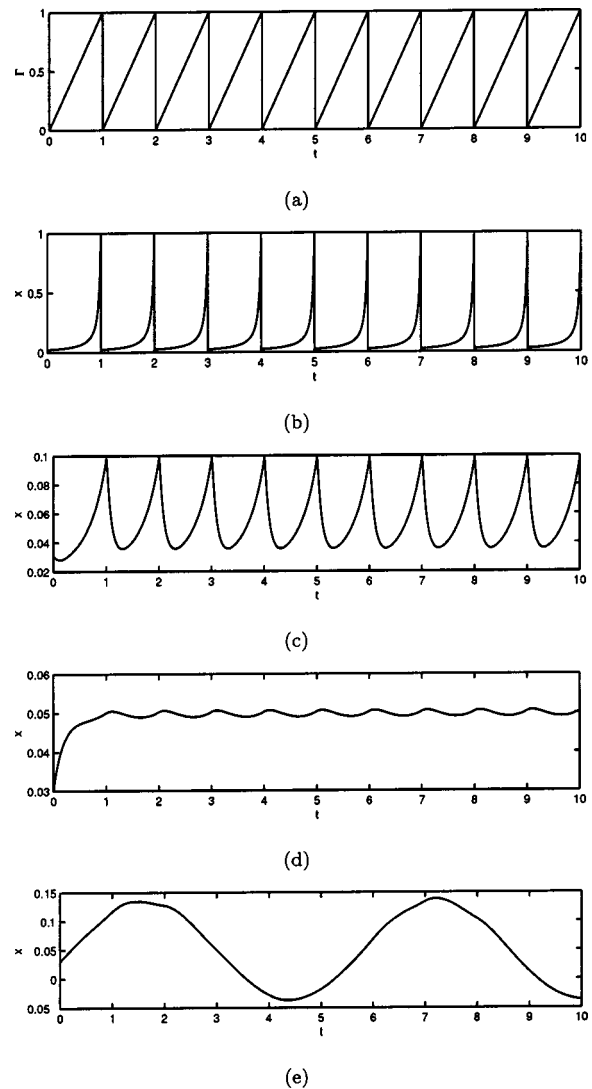

FIG. 5. Dynamics of the pendant drop: oscillator model. (a) Dynamics of surfactant surface concentration; (b) slow reaction, $R/R_0 = 1$; (c) fast reaction, $R/R_0 = 100$; (d) very fast reaction, $R/R_0 = 2000$, steady tip-streaming; (e) very fast reaction, $R/R_0 = 2000$, negligible dissipation.

tion period and wave form of these oscillations are well modeled by (11) with the appropriate choice of parameters, as in Fig. 5(b). As one can observe, this simple nonlinear oscillator model is capable of capturing qualitatively all four regimes of the pendant drop dynamics observed experimentally. In addition to the general dynamics inferred from the model, further simple reasoning leads to the following *crite-*
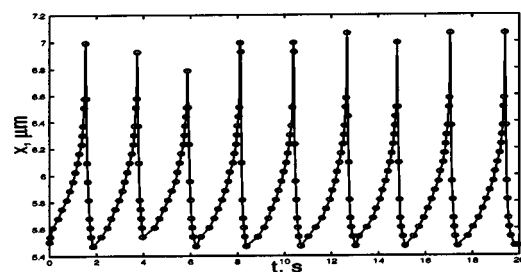

FIG. 6. Experimental data on the tip dynamics (courtesy of J. Fernandez).

Phys. Fluids, Vol. 16, No. 7, July 2004

On physical mechanisms   2561

ria: the oscillatory motion occurs if either: (a) the shear rate is strong enough to lead to formation of a cone and bursting, so that the interface concentration becomes locally dilute and thus is able to accumulate new surfactant molecules, or (b) the reaction is not too fast, so that within the time of filling the interface with new molecules, the new Marangoni flow is developed with sufficient shear rate.

B. Self-similar solution for a steady tip-streaming regime

While in the general case of nonlinear oscillations it is not feasible to obtain analytical solutions, the case of steady tip-streaming admits a significant simplification due to the existence of self-similarity in view of the nearly perfect conical shape of the pendant drops (analogous to that of Taylor cones).[16] This solution can also be interpreted as intermediate asymptotics for other regimes when tip-streaming is observed, since for the period of time when small droplets are emitted the pendant drop takes a conical shape.

Since the experimental observations suggest that the solution behaves in a self-similar fashion, we ground our analysis on this assumption, which is equivalent to seeking solution of the Navier–Stokes equations of the form given by Eq. (17) below. This form must also be compatible with the boundary conditions, including conditions at the interface. While the details are omitted, it is easy to demonstrate that strict similarity requires media of equal densities, and either $\sigma \equiv 0$ or $\sigma \sim z^{-1}$. Therefore, by the transformation $p_i = Bo_i \cdot z + \tilde{p}_i$, $i = 1,2$, one scales out the hydrostatic component of the pressure. Also, for simplicity, we disregard the inertia effects in the water phase since we are interested in the flow pattern in the oil phase, and consider

$$We_1, We_2 \ll 1, \tag{16}$$

so that one can work with the Stokes approximation in both phases. However, accounting for nonlinear inertia effects, which are present in our case since $We_w = 10^4$, is straightforward with the only difference that the solution can be found only numerically: one needs only to remark that for high enough Weber numbers one can expect nonexistence of a self-similar solution in view of generation of swirl such as in the Taylor cone problem.[34,35]

Under these conditions, the self-similar solution is defined by

$$\Psi = r\psi(x), \quad \sigma = \frac{\epsilon}{r}; \quad p = \frac{\pi(x)}{r^2}, \tag{17}$$

where, as will be shown below, $\epsilon = \sigma_{\min}$, $x = \cos\theta$, and Ψ is a Stokes stream function in a spherical coordinates (refer to Fig. 7)

$$x' = r\sin\theta\cos\varphi, \quad y' = \sin\theta\sin\varphi, \quad z' = r\cos\theta, \tag{18}$$

with $\theta \in [0,\pi]$, $\varphi \in [0,2\pi]$. As one can notice, it belongs to the class of convergent flows, such as Jeffrey-Hamel and Taylor cone solutions, but the interfacial tension gradient effect leads to significantly different boundary conditions. In practice, there is always some deviation from self-similarity, but it can be constructed via perturbation expansions in terms
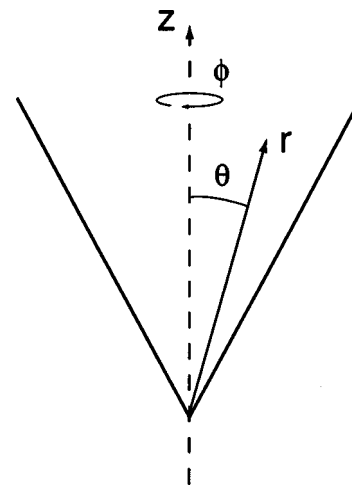

FIG. 7. System of coordinates.

of variations of δBo and $\delta\sigma$. Also, the particular form of the interfacial tension dependence is an idealization of reality and suggested by the experimentally observed self-similar behavior: variable rates chemical reaction along with convection creates a distribution of σ close to (17). Deviations from this law can be accounted for asymptotically through actual material behavior and surfactant transport equations. However, here we are interested in the fundamental structure of the solution and thus we do not account for these adjustments. The most important deviation from self-similarity is due to its breakup, which inevitably takes place since (17) is unbounded as $z \to 0$. Nature, as one can infer from experiments, usually resolves this singularity either by forming a rounded tip [cf. Fig. 1(b)], when capillary forces dominate shear stresses, or by forming a thread [cf. Fig. 1(c)], when shear stresses dominate capillarity. Since surface tension is always bounded, $\sigma_{\min} < \sigma < \sigma_{\max}$ (cf. Fig. 4), the solution (17) breaks down when $z \sim O(\sigma_{\min})$.

Substitution of (17) reduces the standard biharmonic equation for Ψ to

$$(1-x^2)\psi^{(4)} - 4x\psi^{(3)} = 0. \tag{19}$$

Since twice the mean curvature equals

$$\frac{1}{R_1} + \frac{1}{R_2} = \frac{\cot\Theta}{r}, \tag{20}$$

where Θ is a cone angle, the dynamic boundary conditions yield ($\xi = \cos\Theta$)

$$[\pi(\xi)] - \frac{\epsilon\xi}{\sqrt{1-\xi^2}} = -\frac{2\xi}{1-\xi^2}[\psi(\xi)], \tag{21}$$

$$\epsilon = -\frac{2}{\sqrt{1-\xi^2}}[\psi(\xi)] - \sqrt{1-\xi^2}[\psi''(\xi)], \tag{22}$$

with the pressure given by

$$\pi(\xi) = \xi\psi''(\xi) - \frac{1-\xi^2}{2}\psi^{(3)}(\xi), \tag{23}$$

or $\pi'(\xi)=\psi''(\xi)$. The system is completed with velocity continuity conditions

$$\psi_1(\xi)=\delta\psi_2(\xi), \tag{24}$$

$$\psi_1'(\xi)=\delta\psi_2'(\xi), \tag{25}$$

where $\delta=\sqrt{\mathrm{We}_2/\mathrm{We}_1}$ and zero stream function locus

$$x=1: \quad \psi_2=0, \tag{26}$$

$$x=-1: \quad \psi_1=0, \tag{27}$$

$$x=\xi: \quad \psi_1=\psi_2=0. \tag{28}$$

The kinematic condition is trivial and contained in the above conditions for $x=\xi$ (cone surface). Integrating Eq. (19) three times yields

$$(x^2-1)\psi'-2x\psi=C_0+C_1x+C_2x^2, \tag{29}$$

the solution of which is given by

$$\psi=C(x^2-1)+(x^2-1)\int_0^x \frac{C_0+C_1\tilde{x}+C_2\tilde{x}^2}{(\tilde{x}^2-1)^2}\,d\tilde{x}. \tag{30}$$

Application of the boundary conditions gives the final solution

$$\psi_1=-\frac{\epsilon}{2}\left\{\frac{(x+1)(x-\xi)(\xi-1)[-2\xi(1+\xi)+\delta(-1+2\xi^2)]}{\sqrt{1-\xi^2}[1+\xi+\delta(1-\xi)]}+\xi(x^2-1)\sqrt{1-\xi^2}\log\left(\frac{x+1}{x-1}\frac{\xi-1}{\xi+1}\right)\right\}, \tag{31}$$

$$\psi_2=-\epsilon\frac{(x-1)(x-\xi)(2\xi^2+\xi-1)}{2\sqrt{1-\xi^2}[1+\xi+\delta(1-\xi)]}. \tag{32}$$

The streamlines are as shown in Fig. 8.

The existence of self-similar solution (17) provides direct support for the proposed mechanism for self-sustained Marangoni phenomena and emphasizes that the conical shape of the pendant drop is a dynamic effect as opposed to Taylor cones, which are static. The slight divergence of the streamlines from the axis of symmetry away from the cone tip is due to viscous diffusion. One might conjecture that this streamline divergence may be responsible for the observed droplet trajectory splitting. However, the same diffusive effect must take place in tip-streaming experiments with externally imposed flows, but no trajectory splitting has been observed (cf. Ref. 8). Thus, there must be some other mechanism responsible for that, which will be discussed in Sec. III.

III. DROPLET DYNAMICS

The system under consideration is a water drop pendant in the oil phase with an acid-base reaction at the oil–water interface. Here we would like to unravel the primary mechanisms that distinguish the phenomena of tip-streaming in this case from the standard one occurring in shear or extensional flows. Two primary differences—the absence of an independent external flow and the presence of a chemical reaction—are responsible for the flow pattern shown in Fig. 9. While the origin of the flow along the interface and axis of symmetry is discussed in Sec. I, the observed droplet trajectory splitting (cf. Fig. 9) is not explained by the generated flow since the angle of the cone, in which the droplet trajectories lie, is of the same order as the pendant drop cone angle $\sim78°$ (see Fig. 5 in Ref. 1). Indeed, the generated Marangoni flow shown in Figs. 8 and 9 diverges insufficiently in order to explain the much stronger sideways motion of the droplets, which depart from axis in a very organized fashion—one drop moves to the left, the next one moves to
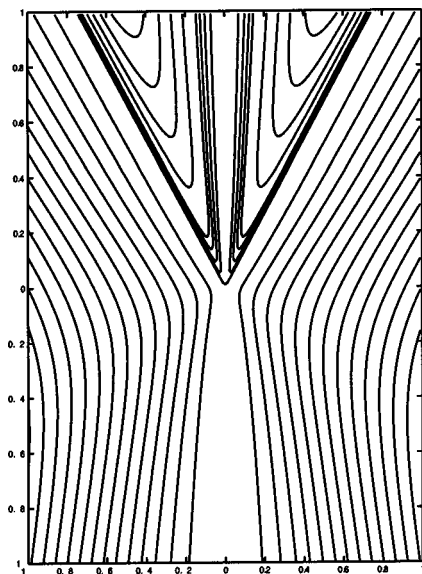
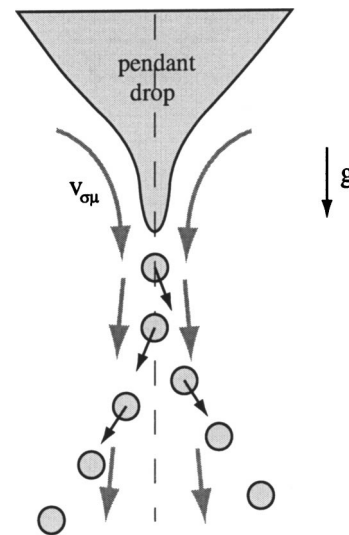FIG. 8. Streamlines in a Stokes regime.

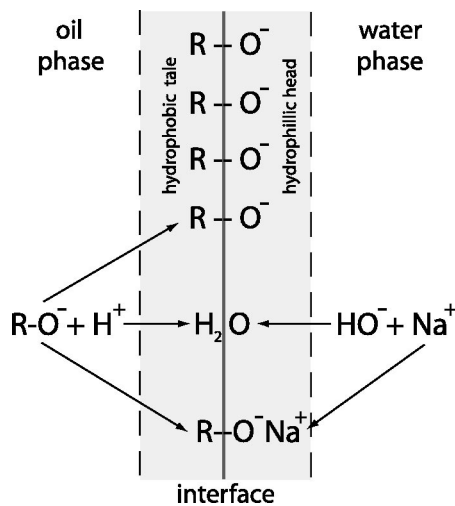FIG. 9. Schematics of the droplets splitting phenomena.

FIG. 10. Basic chemical features of the problem: acid-base reaction at the oil–water interface.

the right—thus demonstrating the existence of a force different from both gravity and hydrodynamic drag. At the same time, the low Reynolds number of the flow in the oil phase, $Re_o \simeq 0.2$, seems to exclude the possibility of swirling motion outside the cone, which also could potentially lead to the droplets splitting. It should be noted that the transition to swirling motion found inside Taylor cones (cf. Ref. 35) takes place at sufficiently high Reynolds numbers. In addition, careful viewing of the flow visualizations reported in Ref. 1 clearly demonstrate that the droplets' trajectories are straight, thus indicating the absence of any swirling. Therefore, here we consider an alternative mechanism for the droplet trajectory splitting.

The velocity of the droplets has two origins: one is due to Marangoni convection and the other is due to an unspecified repulsive force (the role of gravity is negligible here). As it will be shown, this force takes its origin in the electrostatic interaction induced by the ionic nature of surfactant. For an exact calculation of the forces involved in this phenomenon, one needs to solve a complete hydroelectro-chemical problem. However, if one is just interested in orders of magnitude, the problem admits a very simple analysis which is given below.

While the details on the chemistry of the reaction at the oil–water interface between linoleic (fatty) acid and sodium hydroxide can be found in Ref. 36, we provide some basic facts sufficient for understanding the electrostatic aspects of phenomena (cf. Fig. 10). The reaction is

$$RO^- + H^+ + Na^+ + HO^- \rightarrow H_2O + RO^-Na^+, \qquad (33)$$
$$\underset{\text{linoleic acid}}{} \quad \underset{\text{sodium hydroxide}}{}$$
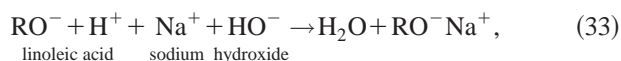
where it is assumed that recombination of H^+ and HO^- and that of Na^+ and RO^- dominate any others. In particular, the last interfacial reaction produces a tight, undissociated sodium salt, so that the insoluble surfactant becomes surface inactive. This salt partially remains at the interface and partially diffuses into the oil phase. Reaction (33) is, on one hand, responsible for the substantial variation of interfacial tension (from 35.0 mN/m for clean interface case to the low

magnitude 1–2 mN/m; see Ref. 36 and references therein). This in turn allows the Marangoni stresses to create substantial shear flow along the interface as sketched in Fig. 9. On the other hand, the effect of the reaction is the formation of a double layer at the oil–water interface. Its existence has been envisaged by Risenfeld,[37] but its mathematical theory was developed much later (cf. Guoy,[38] Chapman,[39] and Debuy and Hükel).[40] We refer the reader to these works (or standard text on physical chemistry of surfaces[41]) for the details, and below provide just the physical discussion of this theory as applied to our system. For convenience of the subsequent analysis we summarize the relevant electrokinetic constants in Table II.

Since the hydrogen cation H^+ and hydroxyl ion HO^- have the highest mobilities (and thus diffusion rates), and their recombination rate is much higher than that of anionic surfactant and sodium ion, there is an excess of negative ions, RO^-, in the oil phase and interface and positive ions, Na^+, in the water phase, as shown in Fig. 11. The last process is usually referred to as a *polarization* of the interface or formation of a double layer. The much lower recombination rate of RO^- and Na^+ comes from the phenomenon of hydration—formation of a shell of water molecules around sodium ions. Thus, the characteristic reaction rate of the whole system is controlled by the slowest reaction (which is a recombination of acid radicals and sodium ions) and as a result the properties of the double layer can be determined from the dynamics of these two types of ions. Consider, for definiteness, the water phase. In the steady state the diffusion flux balances the flux driven by electrostatic interactions:

$$C_{Na^+} b_{Na^+} \frac{\delta\varphi^w}{\delta x} \sim D_{Na^+} \frac{\delta C_{Na^+}}{\delta x^2}, \qquad (34)$$

TABLE II. Electrokinetic constants.

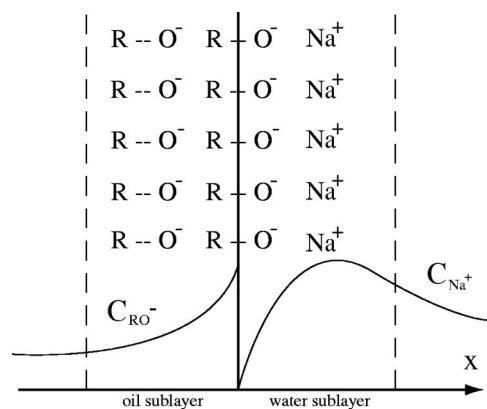|	
Mobility of b_{H^+}	3.26×10^{-3} cm²/s V
Mobility of b_{HO^-}	1.80×10^{-3} cm²/s V
Mobility of b_{Na^+}	$b_{Na^+} = 0.45 \times 10^{-3}$ cm²/s V
Pendant drop radius R_1	2×10^{-4} m
Droplet radius R_2	3×10^{-6} m

FIG. 11. Double layer structure.

where the potential φ^w is governed by the Gauss theorem relating the divergence of the gradient of the electrical potential φ at a given point to the charge density at that point

$$\frac{\delta \varphi^w}{\delta x^2} \sim -\frac{e}{\epsilon_0 \epsilon^w}[C_{Na^+} - C_{HO^-}]. \tag{35}$$

In view of the high mobility of C_{HO^-}, one can neglect the concentration variation of these ions in the double layer, so that $C_{Na^+} - C_{HO^-}$ is controlled by the variation of the concentration of sodium ions $C_{Na^+} - C_{HO^-} \sim C_{Na^+}^\infty - \delta C_{Na^+} - C_{HO^-}^\infty + \delta C_{HO^-} \simeq -\delta C_{Na^+}$, as shown in Fig. 11. The form of the concentration profile for C_{Na^+} follows from the fact that the reaction is diffusion controlled, i.e., ions approaching the interface react instantaneously compared to the characteristic time of diffusion. Therefore, the magnitude of concentration at the interface is close to zero, so that the concentration variation in a double layer $\delta C_{Na^+} \sim C_{Na^+}$. Taking into account the Einstein relation between diffusion coefficient and mobility $D_{Na^+} = (k_B T/e)b_{Na^+}$, and excluding electric potential variation, one arrives at the following estimates for the double layer thicknesses:

$$\delta x \sim h^w \sim \left[\frac{\epsilon_0 \epsilon^w}{e^2} \frac{k_B T}{C_{Na^+}^\infty}\right]^{1/2} \sim 10^{-8} \text{ m.} \tag{36}$$

For reference, the average distance between ions in the water phase is $\langle d^w \rangle_C = (C_{NaOH} N_A)^{-1/3} \sim 10^{-8}$ m, while the average distance between surfactant molecules at the interface $\langle d^w \rangle_\Gamma = (\Gamma_{RO^-} N_A)^{-1/2} \sim 10^{-9}$ m. The fact that $h^w \sim \langle d^w \rangle_C$ has the following explanation. Estimates (36) provide just the characteristic length scale, but in reality, the thickness of the double layer is several times greater than just the average distance between ions. Also, the very high surface charge density $\Gamma_{RO^-} N_A e \sim 1$ C/m^2 cannot be neutralized just by $h^w C_{Na^+} N_A e \sim 1.5 \times 10^{-2}$ C/m^2, and thus leads to an increase of density of sodium ions Na$^+$ in the double layer compared to $C_{Na^+}^\infty$, as sketched in Fig. 11 and a thickening of the double layer.

The presence of the double layer at the interface leads to electrostatic dipole–dipole type interactions between the pendant drop of radius R_1 and small droplets of radius R_2, and between the small droplets themselves. Conceptually we follow the approach of Derjaguin and Landau[42] but accounting for the geometry of interacting objects (instead of the planar geometry assumed in Ref. 42). This interaction can be represented as a force between two pairs of concentric hemispheres, each of which carries opposite charges as shown in Fig. 12(a). Note that the interaction with the furthest pair of hemispheres (dashed) is significantly weakened in view of high dielectric constant of water and thus omitted in our consideration. Further, each pair of hemispheres can be approximated as a dipole, the moment of which is a product of the double layer thickness and the total charge

$$p_i = 2\pi e R_i^2 \Gamma^{max} N_A h^w, \quad i = 1,2. \tag{37}$$

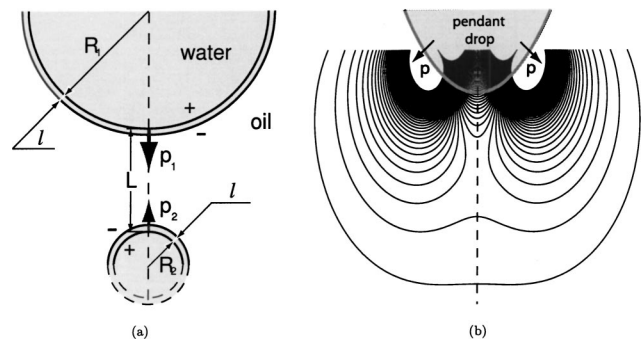The interaction force between two dipoles separated by distance L is therefore

FIG. 12. Basic features of electrostatic interaction.

$$F_{p_1-p_2} = \frac{6}{4\pi\epsilon_0\epsilon^o} \frac{p_1 p_2}{L^4}. \tag{38}$$

Two major effects in our particular case lead to this force being significant: the high dielectric constant of water increases the thickness of the double layer and therefore its dipole moment, while the low dielectric constant of the oil increases the interaction force between dipoles. Since $F_{p_1-p_2} \sim R_1^2 R_2^2/L^4$ the force $F_{p_1-p_2}$ of interaction between a small droplet of radius R_2, and pendant drop, $R_1 \gg R_2$, at $L \sim R_1$, is weaker than that $F_{p_2-p_2}$ between the small droplets of the same radius R_2 at $L \sim R_2$. Quantitatively,

$$F_{p_1-p_2} \sim 0.5 \times 10^{-7} \text{ N,} \tag{39}$$

while the force between droplets should be evaluated for $L \sim 4R_2$, as observed in experiments, and yields

$$F_{p_2-p_2} \sim 1.0 \times 10^{-6} \text{ N.} \tag{40}$$

The Stokes drag experienced by droplets due to a sideways motion may be estimated from Stokes' law and the experimentally observed velocity as

$$F_{St} \sim 6\pi\mu^o R_2 v_{\sigma\mu} \sim 0.5 \times 10^{-6} \text{ N,} \tag{41}$$

i.e., comparable with (39)–(40).[43] In this context, the well-organized droplet motion has the following explanation: the isopotentials of the electric field of the pendant drop, shown in Fig. 12(b) for the case when the tip of the drop is free of surfactant, indicate that the axis corresponds to the local maximum of electric strength $E = -\nabla\varphi$, so that any charged object will tend to move away from the axis of symmetry in a manner analogous to the behavior of a point mass in unstable maximum of potential energy. Furthermore, the small droplets also experience repulsive interactions, which therefore provide a mechanism selecting the direction of a sideways motion of each droplet. Thus in our system the long range dipole–dipole interaction exhibits itself in a dynamic manner. The static analog of long-range algebraic dipolar interaction is known in two-dimensional colloidal crystals[44] when polystyrene spheres trapped at water–air interface are organized due to dissociation of the sulfonic acid groups and appearance of the dipoles in view of screening water molecules. In other circumstances this mechanism is responsible for the stability of water-in-oil emulsions.

While the outline of the basic mechanism provided here has very sound support, it is based on the assumption of the exclusive role of electrostatic interactions in creating the

Phys. Fluids, Vol. 16, No. 7, July 2004

On physical mechanisms   2565

sideways motion of small droplets. The structure of the double layer suggests another contributing mechanism, however: the Marangoni flow along the interface can convect negative charges, the presence of which in the axial flow will lead to a sideways motion of the bulk. It may also happen that although small droplets carry some excess of positive charge immediately after ejection, it will be neutralized by adsorbing surfactant ions from the bulk.

IV. SUMMARY AND CONCLUSIONS

In this paper we have considered plausible models for the observations in Ref. 1. In particular, the role of Marangoni stresses in driving and sustaining nonlinear periodic motion of a pendant drop is clarified and well supported by: (i) the existence of self-similar solution for a steady tip-streaming regime and (ii) the qualitative prediction of the experimentally observed modes of tip-streaming by the relaxation oscillator model embodying the basic Marangoni mechanism. The formation of a spray cone is found to be consistent with the repulsive electrostatic dipole–dipole interactions originating from the ionic nature of the surfactant.

In summary, we would like to emphasize a peculiarity of the phenomena. First of all, the size of the pendant drop is such that the chemical energy generated at the interface is sufficient to drive a significant Marangoni flow, which leads to a pointed conical shape of pendant drop. In view of surface tension boundedness (capillary pressure cannot support the dynamic pressure) the pointed end emits droplets, the small size of which is explained by the capillary breakup with surfactant gradients. This phenomenon of tip-streaming is a singular removal of the surfactant from the interface responsible for periodicity of the phenomenon. Second, the electrostatic interactions create a specific flow pattern in which repulsion is sufficient to equilibrate with Stokes drag (in view of small enough droplet size). In closing it should be noted that both conical pendant drop and spray cone formation are dynamic effects as opposed to the well-known static Taylor cone and colloidal crystal formation,[44] the latter of which is also due to dipole–dipole type of interaction as the spray cone pattern in our case.[45,46]

ACKNOWLEDGMENTS

formed by H. Wong, D. Rumschitzki, and C. Maldarelli ["Marangoni effects on the motion of an expanding or contracting bubble pinned at a submerged tube tip," J. Fluid Mech. **379**, 279 (1999)]. It was found that the Marangoni flow induced by concentration gradients reduces this gradient and maintains a uniform distribution of surfactant, while the enhanced tangential flow violates the second assumption. In any case, our situation involves a tip-streaming phenomenon which allows for self-sustained concentration gradients and the Marangoni flow in this case plays an opposite role—it maintains the concentration gradients thus contradicting the first assumption as well.

[7] G. I. Taylor, "The formation of emulsions in definable fields of flow," Proc. R. Soc. London, Ser. A **146**, 501 (1934).

[8] H. A. Stone, "Dynamics of drop deformation and breakup in viscous fluids," Annu. Rev. Fluid Mech. **26**, 65 (1994).

[9] R. A. de Bruijn, "Tipstreaming of drops in simple shear flows," Chem. Eng. Sci. **48**, 277 (1993).

[10] M. Siegel, "Influence of surfactant on rounded and pointed bubbles in two-dimensional Stokes flow," SIAM (Soc. Ind. Appl. Math.) J. Appl. Math. **59**, 1998 (1999).

[11] Y. T. Hu, D. J. Pine, and L. G. Leal, "Drop deformation, breakup, and coalescence with compatibilizer," Phys. Fluids **12**, 484 (2000).

[12] A. Acrivos and T. S. Lo, "Deformation and breakup of a single slender drop in an extensional flow," J. Fluid Mech. **86**, 641 (1978).

[13] C. D. Eggleton, Y. P. Pawar, and K. J. Stebe, "Insoluble surfactants on a drop in an extensional flow: a generalization of the stagnated surface limit to deforming interfaces," J. Fluid Mech. **385**, 79 (1999).

[14] C. D. Eggleton, T.-M. Tsai, and K. J. Stebe, "Tip-streaming from a drop in the presence of surfactants," Phys. Rev. Lett. **87**, 048302 (2001).

[15] G. I. Taylor, "Disintegration of water drops in an electric field," Proc. R. Soc. London, Ser. A **280**, 383 (1964).

[16] G. I. Taylor, "Conical free surfaces and fluid interfaces," Proceedings 11th International Congress on Applied Mechanics, Munich, 1964, pp. 191–219.

[17] L. Hayati, A. I. Bailey, and Th. F. Tadros, "Mechanism of stable jet formation in electrohydrodynamic atomization," Nature (London) **319**, 41 (1986).

[18] M. Dupeyrat and E. Nakache, "Direct conversion of chemical energy into mechanical energy at an oil water interface," Bioelectrochem. Bioenerg. **5**, 134 (1978).

[19] N. Magome and K. Yoshikawa, "Nonlinear oscillations and ameba-like motion in an oil/water system," J. Phys. Chem. **100**, 19102 (1996).

[20] N. M. Kovalchuk and D. Vollhardt, "Auto-oscillations of surface tension," Phys. Rev. E **60**, 2029 (1999).

[21] G. Gouesbet, "Simple-model for bifurcations ranging up to chaos in thermal lens oscillations and associated phenomena," Phys. Rev. A **42**, 5928 (1990).

[22] R. S. Shaw, *The Dripping Faucet as a Model Chaotic System* (Arial, Santa Cruz, CA, 1984).

[23] P. Martien, S. C. Pope, P. L. Scott, and R. S. Shaw, "The chaotic behavior of the leaky faucet," Phys. Lett. **110A**, 399 (1985).

[24] O. E. Rössler, "Continuous chaos," in *Synergetics, A Workshop*, edited by H. Haken (Springer, Berlin, 1977), pp. 174–183.

[25] A. de Innocento and L. Renna, "Dripping faucet," Int. J. Theor. Phys. **35**, 941 (1996).

[26] Even the static case of the dripping faucet problem represents a very rich and complex subject [see C. S. Riera and E. Risler, "Axisymmetric capillary surfaces as a dynamical system," Nonlinearity **15**, 1843 (2002), and references therein].

[27] B. Ambravaeswaran, S. D. Phillips, and O. A. Basaran, "Theoretical analysis of a dripping faucet," Phys. Rev. Lett. **85**, 5332 (2000).

[28] N. Fuchikami, S. Ishioka, and K. Kiyono, "Simulation of a dripping faucet," J. Phys. Soc. Jpn. **68**, 1185 (1999).

[29] P. Coullet, L. Mahadevan, and C. Riera, "Return map for the chaotic dripping faucet," Prog. Theor. Phys. Suppl. **139**, 507 (2000).

[30] R. P. Borwankar and D. T. Wasan, "The kinetics of adsorption of surface-active agents at gas–liquid surfaces," Chem. Eng. Sci. **38**, 1637 (1983).

[31] Y. Gu and D. Li, "A model for a liquid drop spreading on a solid surface," Colloids Surf., A **142**, 243 (1998).

[32] A. Nadim and B. M. Rush, "Mechanisms contributing to the damping of shape oscillations of liquid drops," Third International Conference on Multiphase Flow, ICMF'98, Lyon, France, June 8–12 1998.

[33] We have used other state equations with the same net qualitative behavior.

[1] J. M. Fernandez and G. M. Homsy, "Chemical reaction-driven tip-streaming phenomena in a pendant drop," Phys. Fluids **16**, 2548 (2004).

[2] F. Squires, U.S. Patent No. 1238355 (1917).

[3] F. G. Donnan, "Über die Natur der Seifenemulsionen," Z. Phys. Chem. **31**, 42 (1899).

[4] J. M. Andreas, E. A. Hauser, and W. B. Tucker, "Boundary tension by pendant drop," J. Phys. Chem. **42**, 1001 (1938).

[5] Y. Touhami, G. H. Neale, V. Hornof, and H. Khalfalah, "A modified pendant drop method for transient and dynamic interfacial tension measurement," Colloids Surf., A **112**, 31 (1996).

[6] A study of the two central assumptions made in the pendant drop method, those of uniform surfactant concentration and purely radial flow was per-

[34]M. A. Goldshtik and V. N. Shtern, "Collapse in conical viscous flows," J. Fluid Mech. **218**, 483 (1990).

[35]V. Shtern, M. Goldshtik, and F. Hussain, "Generation of swirl due to symmetry breaking," Phys. Rev. E **49**, 2881 (1994).

[36]C. I. Chiwetelu, V. Hornof, and G. H. Neale, "Interaction of aqueous caustic with acidic oils," J. Can. Pet. Technol. **28**, 71 (1989).

[37]E. H. Risenfeld, "Concentrationketten mit nichtmischbaren Lösungsmitteln," Ann. Phys. (Leipzig) **8**, 616 (1902).

[38]G. Gouy, "Sur la constitution de la charge lectrique la surface d'un lectrolyte," J. Phys. **9**, 457 (1910).

[39]D. L. Chapman, "A contribution to the theory of electrocapillarity," Philos. Mag. **25**, 475 (1913).

[40]P. Debye and E. Hückel, "Zur theorie der elektrolyte. I. Gefrierpunktserniedrigung und verwandte Erscheinungen," Phys. Z. **24**, 185 (1923).

[41]A. W. Adamson and A. P. Gast, *Physical Chemistry of Surfaces* (Wiley-Interscience, New York, 1997).

[42]B. Derjagiun and L. Landau, "Theory of the stability of strongly charged lyophobic sols and of the adhesion of strongly charged particles in solutions of electrolytes," Acta Physicochim. URSS **14**, 633 (1941).

[43]It should be noted that constants of the order of unity in force estimates (39)–(41) can be determined only from the solution of the complete problem and are influenced by a particular distribution of the surfactant which in turn is affected by chemical reaction and hydrodynamic motion in both phases ($Re_o \sim 0.2, Re_w \sim 10^4$).

[44]P. Pieranski, "Two-dimensional interfacial colloidal crystals," Phys. Rev. Lett. **45**, 569 (1980).

[45]H. Wang, D. Rumschitzki, and C. Maldarelli, "Marangoni effects on the motion of an expanding or contracting bubble pinned at a submerged tube tip," J. Fluid Mech. **379**, 279 (1999).

[46]C. S. Riera and E. Risler, "Axisymmetric capillary surfaces as a dynamical system," Nonlinearity **15**, 1843 (2002).